IJCRT.ORG ISSN : 2320-2882

INTERNATIONAL JOURNAL OF CREATIVE RESEARCH THOUGHTS (IJCRT)

An International Open Access, Peer-reviewed, Refereed Journal

Formulation, Optimization and Evaluation of Terbinafine Hydrochloride-Loaded Ethosomal Gel for Topical Antifungal Therapy

Pratibha M. Kore*, Dr. M. S. Kalshetti

M. Pharm., Pharmaceutical Quality Assurance

D.S.T.S. Mandal's College of Pharmacy, Solapur, Maharashtra, India

ABSTRACT

Terbinafine hydrochloride, a first-line allylamine antifungal, shows limited clinical benefit from conventional topical vehicles because of poor stratum corneum permeability and low local bioavailability. This study aimed to design an ethosomal gel of terbinafine hydrochloride to improve cutaneous drug delivery for dermatophyte infections. Ethosomal vesicles were prepared by the cold method and optimized using a 3^2 factorial design with soya lecithin (X1) and ethanol (X2) as independent variables, and entrapment efficiency and particle size as dependent responses. Nine batches (F1–F9) were evaluated for entrapment efficiency, vesicle size, zeta potential, polydispersity index, morphology (TEM) and in vitro release. The optimized batch (F6: 30 mg/mL soya lecithin, 12% v/v ethanol) showed 94.33% entrapment efficiency, a mean vesicle size of 235.61 nm, zeta potential of –38.44 mV and PDI of 0.258, and its release profile fitted best to the Higuchi model (R^2 = 0.9869), consistent with diffusion-controlled release. F6 was incorporated into a Carbopol 940 gel base. The resulting ethosomal gel was off-white, smooth and homogeneous, with pH 6.18, viscosity 4125.6 cP, spreadability 38.24 g·cm/s, extrudability 96.76% and drug content 97.89%, and released 94.76% of the drug over 12 h in a biphasic pattern. One-month accelerated and real-time stability studies showed less than 2% change in entrapment efficiency, drug content and cumulative release, confirming short-term physical and chemical stability. These findings support the ethosomal gel as a promising, patient-friendly platform for enhanced topical delivery of terbinafine hydrochloride, warranting further ex vivo permeation and in vivo evaluation.

Keywords: Terbinafine hydrochloride; Ethosomes; 3^2 factorial design; cold method; topical antifungal gel; sustained drug release

1. INTRODUCTION

The clinical performance of a topical antifungal agent depends as much on its delivery system as on its intrinsic pharmacological activity. Conventional creams, ointments and gels are frequently limited by the barrier function of the stratum corneum, which restricts drug penetration to deeper viable skin layers and, in the case of nail or follicular infections, prevents adequate local drug concentrations from being achieved. Vesicular carriers such as liposomes, niosomes, transfersomes and ethosomes have therefore been explored to overcome this limitation by improving drug partitioning into and across the skin while confining the therapeutic effect to the site of application. [2,3,34]

Ethosomes are soft, malleable phospholipid vesicles containing a relatively high proportion of ethanol (20–45% v/v) together with phospholipid and water. The ethanol fluidizes both the vesicle bilayer and the intercellular lipids of the stratum corneum, allowing the flexible vesicles to penetrate deeper into the skin than conventional liposomes while still protecting the entrapped drug from rapid degradation. This combination of a fluidizing co-solvent and a deformable carrier makes ethosomes particularly attractive for lipophilic, poorly water-soluble actives that must reach the epidermis or dermis to be effective. [3,9,21]

Terbinafine hydrochloride is a broad-spectrum allylamine antifungal that acts by inhibiting fungal squalene epoxidase, thereby blocking ergosterol biosynthesis and causing intracellular squalene accumulation and fungal cell death. It is a Biopharmaceutics Classification System (BCS) class II drug, practically insoluble in water and only slightly soluble in common topical vehicles, and its conventional cream and ointment formulations show restricted penetration through the stratum corneum. This is a particular problem in conditions such as onychomycosis and chronic dermatophytosis, where the drug must reach deeper skin and nail structures. Encapsulating terbinafine hydrochloride within an ethosomal carrier and subsequently incorporating the vesicles into a semisolid gel base was therefore expected to combine the permeation-enhancing properties of ethosomes with the ease of application, spreadability and patient acceptability of a topical gel, while also providing sustained drug release, reduced dosing frequency and lower risk of the systemic exposure (and associated hepatotoxicity) seen with oral therapy. [2,4]

The present work describes the systematic formulation of terbinafine hydrochloride-loaded ethosomes by the cold method, their optimization using a 3^2 factorial design, selection of an optimized batch based on entrapment efficiency, particle size, zeta potential and in vitro release, incorporation of the optimized ethosomes into a Carbopol 940 gel, and full physicochemical, release-kinetic and short-term stability evaluation of the resulting ethosomal gel. [5,9,21,33]

2. MATERIALS AND METHODS

2.1 Materials

Terbinafine hydrochloride was procured as a gift sample from Solanki Enterprises, Pune. Soya lecithin, ethanol, propylene glycol and cholesterol (Sisco Chem Laboratory) were used for ethosome preparation. Carbopol 940, methyl paraben, propyl paraben, propylene glycol and triethanolamine (Research-Lab Fine Chem Industries, Mumbai) were used for gel formulation. All other chemicals and reagents used were of analytical grade.

Sr. No.	Material	Role	Source
1	Terbinafine hydrochloride	Active pharmaceutical ingredient (antifungal)	Solanki Enterprises, Pune
2	Soya lecithin	Vesicle-forming phospholipid	Sisco Chem Laboratory
3	Ethanol	Skin-penetration enhancer / vesicle fluidizer	Sisco Chem Laboratory
4	Propylene glycol	Co-solvent for phospholipid bilayer	Sisco Chem Laboratory
5	Cholesterol	Membrane stabilizer	Sisco Chem Laboratory
6	Carbopol 940	Gelling agent	Research-Lab Fine Chem Industries
7	Methyl / propyl paraben	Preservatives	Research-Lab Fine Chem Industries
8	Triethanolamine	Neutralizing agent	Research-Lab Fine Chem Industries
9	Distilled water	Vehicle	In-house

Table 1. Materials used for preparation of terbinafine hydrochloride-loaded ethosomes and ethosomal gel.

2.2 Preformulation studies

Terbinafine hydrochloride was characterized for organoleptic properties (color, odour, taste) and micromeritic properties (bulk and tapped density, Carr's index, Hausner ratio, angle of repose, coefficient of friction). Aqueous, ethanolic and phosphate-buffer (pH 7.4) solubility was determined by the shake-flask method (orbital shaker, 24 h, 37 °C) followed by UV analysis. Melting point was determined by the capillary method. The wavelength of maximum absorption (λmax) and calibration curves were established in ethanol, phosphate buffer pH 7.4 and distilled water over 2–10 µg/mL. Drug–excipient compatibility was assessed by FTIR (KBr disc method) and thermal behavior by differential scanning calorimetry (DSC; 50–300 °C, 20 °C/min, nitrogen purge).

2.3 Experimental design for ethosome optimization

A 3^2 factorial design was used to optimize the ethosomal formulation, with soya lecithin (X1) and ethanol concentration (X2) as independent variables at three coded levels (–1, 0, +1), giving nine formulations (F1–F9). Entrapment efficiency and particle size were selected as dependent responses and the design was analyzed using Design-Expert® software (v13) under response-surface methodology (quadratic model). [33]

Formulation	Terbinafine HCl (mg)	Soya lecithin (mg)	Cholesterol (mg)	Propylene glycol (mL)	Ethanol (mL)	Water (up to, mL)
F1	15	15	15	3	6	30
F2	15	15	15	3	9	30
F3	15	15	15	3	12	30
F4	15	30	15	3	6	30
F5	15	30	15	3	9	30
F6	15	30	15	3	12	30
F7	15	45	15	3	6	30
F8	15	45	15	3	9	30
F9	15	45	15	3	12	30

Table 2. Composition of the nine ethosomal batches from the 3² factorial design (F1–F9).

2.4 Preparation of ethosomes (cold method)

Soya lecithin, cholesterol and terbinafine hydrochloride were dissolved in ethanol with magnetic stirring (700 rpm, 30 °C); propylene glycol was added gradually to this organic phase. Distilled water, pre-warmed to 30 °C, was added slowly to the stirred organic phase, and stirring was continued for a further 30 min to yield a homogeneous ethosomal suspension, which was cooled to room temperature and stored under refrigeration.

2.5 Evaluation of terbinafine hydrochloride-loaded ethosomes

Entrapment efficiency was determined indirectly by ultracentrifugation of the ethosomal dispersion (5 mL phosphate buffer pH 7.4, 1 h), with the unentrapped drug in the supernatant assayed at 208.5 nm. Mean particle size, polydispersity index (PDI) and zeta potential were measured by dynamic light scattering (Malvern Zetasizer, 25 °C, 1:1 ethanol–water dilution). Vesicle morphology of the optimized batch was examined by transmission electron microscopy (TEM; JEOL JEM-2100 Plus) after negative staining. In vitro drug release was studied using a dialysis-bag (12–14 kDa cut-off) method against phosphate buffer pH 7.4 (37 ± 0.5 °C, 50–100 rpm) over 12 h, with samples assayed at 208.5 nm and cumulative percentage release plotted against time. Release data were fitted to zero-order, first-order, Higuchi, Hixson–Crowell and Korsmeyer–Peppas models, and the model with the highest correlation coefficient (R^2) was taken as best describing the release mechanism. Statistical significance of the factorial model was assessed by ANOVA ($p < 0.05$ considered significant), and model adequacy by R^2, adjusted R^2, predicted R^2 and adequate precision (>4 desirable). [57-60]

2.6 Selection and characterization of the optimized batch

The batch with the most favorable combination of high entrapment efficiency, small particle size, high (negative) zeta potential and low PDI was selected as the optimized batch and further characterized for solubility (shake-flask method in distilled water, ethanol and phosphate buffer pH 7.4), FTIR and DSC. Short-term accelerated stability (40 ± 2 °C/75 ± 5% RH, 1 month; sampling at 0, 15 and 30 days) was assessed by monitoring entrapment efficiency and in vitro release.

2.7 Preparation of the ethosomal gel

Carbopol 940 was hydrated in purified water for 1–2 h and neutralized with triethanolamine to a skin-compatible pH (~7–7.4). Methyl and propyl paraben, pre-dissolved in warm water, were incorporated as preservatives, followed by the optimized (F6) ethosomal suspension, with continuous stirring until a smooth, homogeneous, bubble-free gel was obtained. [55]

Sr. No.	Ingredient	Quantity
1	Terbinafine hydrochloride ethosomes (F6)	30 mL
2	Carbopol 940	0.10 g
3	Triethanolamine	0.2 mL
4	Methyl paraben	0.06 g
5	Propyl paraben	0.02 g
6	Distilled water	q.s.

Table 3. Composition of the optimized terbinafine hydrochloride-loaded ethosomal gel.

2.8 Evaluation of the ethosomal gel

The gel was evaluated for organoleptic properties, pH (digital pH meter, 1% w/v aqueous dispersion), viscosity (Brookfield viscometer, spindle 64), spreadability (parallel-plate method), extrudability (collapsible tube method, 15 g load), drug content uniformity (UV, 211 nm) and in vitro release (Franz diffusion cell, dialysis membrane, phosphate buffer pH 7.4 receptor, 37 °C, 75 rpm, sampling at 0–5 h). Short-term stability (25 ± 2 °C/60% RH, 1 month) was assessed for organoleptic properties, pH, viscosity, spreadability, drug content and cumulative drug release at 0, 15 and 30 days. [5,22-24,55]

3. RESULTS AND DISCUSSION

3.1 Preformulation studies

Terbinafine hydrochloride was a white to off-white, odourless, bitter powder. Micromeritic evaluation indicated poor flow (bulk density 0.285 g/mL, tapped density 0.476 g/mL, Carr's index 40.12%, Hausner ratio 1.67, angle of repose 46.45°, coefficient of friction 1.052), consistent with the need for a liquid/semisolid (vesicular gel) rather than a solid dosage form. The drug showed a melting range of 213–215 °C (literature 209–215 °C), confirming identity and purity. Solubility followed the order ethanol (22.66 µg/mL) > phosphate buffer pH 7.4 (17.91 µg/mL) > distilled water (9.50 µg/mL), i.e. the drug was practically insoluble in water and only slightly soluble in the other media, consistent with its BCS class II character. λmax values of 224 nm (ethanol), 208 nm (phosphate buffer pH 7.4) and 206 nm (distilled water) were used to construct linear calibration curves (R^2 = 0.981–0.989) that were used for all subsequent quantification.

FTIR spectra of the drug alone and in combination with soya lecithin, cholesterol, propylene glycol and as a physical mixture retained all the principal characteristic bands of terbinafine hydrochloride (O–H stretching 3502–3896 cm^{-1}, aliphatic C–H stretching 2854–2924 cm^{-1}, aromatic C=C/C–H bending 1473–1643 cm^{-1} and C–O stretching near 1065 cm^{-1}), with only minor shifts and no loss or emergence of characteristic peaks, indicating the absence of major chemical incompatibility between drug and excipients. DSC of the drug showed a sharp endothermic peak near 210 °C, consistent with its crystalline melting behavior and in agreement with the melting point determined by the capillary method; the physical mixture showed a broadened endotherm (peak 207.5 °C), consistent with partial dilution/interaction typical of a compatible physical blend. [51,52]

3.2 Optimization of ethosomes: entrapment efficiency, particle size, zeta potential and PDI

Entrapment efficiency across the nine factorial batches ranged from 85.78% (F4) to 94.33% (F6), particle size from 235.61 nm (F6) to 262.52 nm (F7), zeta potential from –31.15 mV (F8) to –38.44 mV (F6), and PDI from 0.258 (F6) to 0.310 (F4, F8) (Table 4, Fig. 1). Entrapment efficiency generally increased with ethanol concentration, consistent with the role of ethanol in fluidizing the phospholipid bilayer and facilitating incorporation of the moderately lipophilic drug; particle size showed the opposite trend at high lecithin loading, where vesicle aggregation likely increased mean diameter. All batches showed PDI below 0.31, indicating fairly narrow and reproducible size distributions, and zeta potentials in the range of –31 to –38 mV, indicative of adequate electrostatic repulsion and colloidal stability against aggregation. [21,34,48]

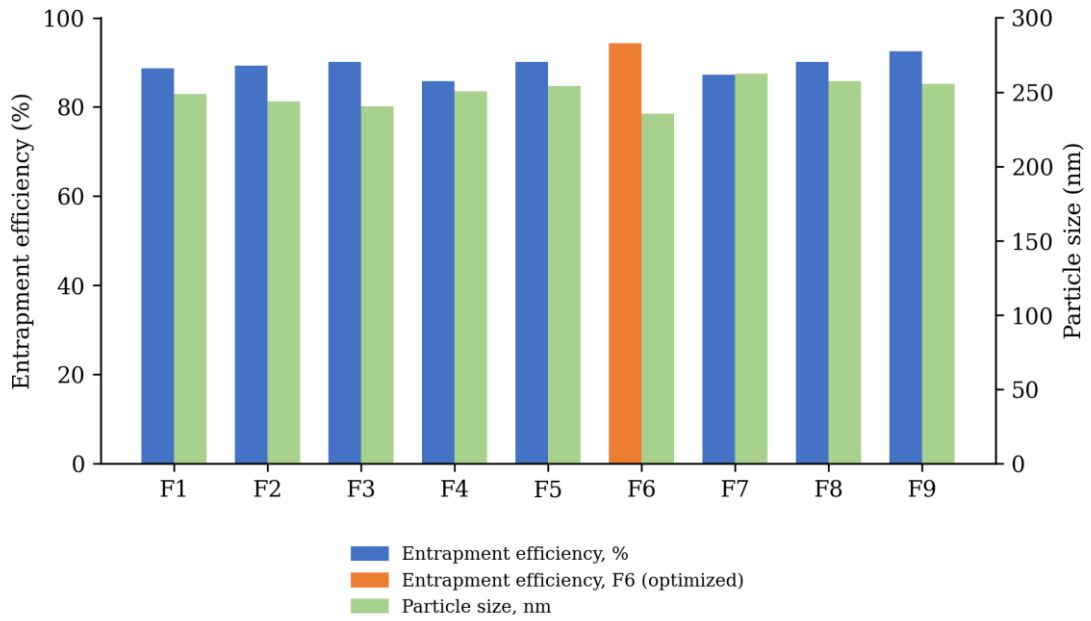

Fig. 1. Entrapment efficiency (%) and particle size (nm) of ethosomal batches F1–F9; F6 (highlighted) combined the highest entrapment efficiency with the smallest particle size.

Batch	Entrapment efficiency (%)	Particle size (nm)	Zeta potential (mV)	PDI
F1	88.66	248.62	–36.73	0.289
F2	89.26	243.67	–34.39	0.270
F3	90.12	240.61	–36.29	0.300
F4	85.78	250.66	–38.18	0.310
F5	90.10	254.29	–37.26	0.272
F6	94.33	235.61	–38.44	0.258
F7	87.27	262.52	–36.29	0.289
F8	90.10	257.30	–31.15	0.310
F9	92.53	255.51	–35.99	0.278

Table 4. Entrapment efficiency, particle size, zeta potential and polydispersity index of ethosomal batches F1–F9.

F6 (30 mg/mL soya lecithin, 12% v/v ethanol) combined the highest entrapment efficiency, smallest and most uniform particle size and most negative zeta potential of the series and was therefore selected as the optimized batch for gel incorporation. TEM images of F6 showed discrete, spherical, unilamellar vesicles

of approximately 240–262 nm, consistent with the DLS size range and confirming a well-formed ethosomal structure.

3.3 Statistical analysis of the factorial design

ANOVA confirmed that the quadratic model was significant for both responses (entrapment efficiency: F = 9.12, p = 0.0152; particle size: F = 9.29, p = 0.0145), with ethanol concentration (B) the dominant significant term for entrapment efficiency (p = 0.0054) and both soya lecithin (A, p = 0.0126) and ethanol (B, p = 0.0470) significant for particle size. Adequate precision ratios of 6.73 (entrapment efficiency) and 8.50 (particle size), both above the desirable threshold of 4, indicated an adequate signal-to-noise ratio for using the models to navigate the design space, supporting F6 as a statistically justified optimum within the studied range.

3.4 In vitro drug release and release kinetics of ethosomes

All nine batches showed sustained, diffusion-type release over 12 h, with cumulative release ranging from 84.4% (F7) to 93.3% (F5); F2, F5 and F6 exceeded 90% release at 12 h (Fig. 2). For the optimized batch F6, the release data fitted best to the Higuchi model (R^2 = 0.9869), followed by the Hixson–Crowell (R^2 = 0.9833), zero-order (R^2 = 0.9255) and first-order (R^2 = 0.8765) models, while the Korsmeyer–Peppas fit was comparatively poor (R^2 = 0.6869) (Table 5, Fig. 3). The strong Higuchi fit indicates that drug release from the ethosomal vesicles is predominantly diffusion-controlled, consistent with a matrix-type release mechanism from the lipid bilayer. [59]

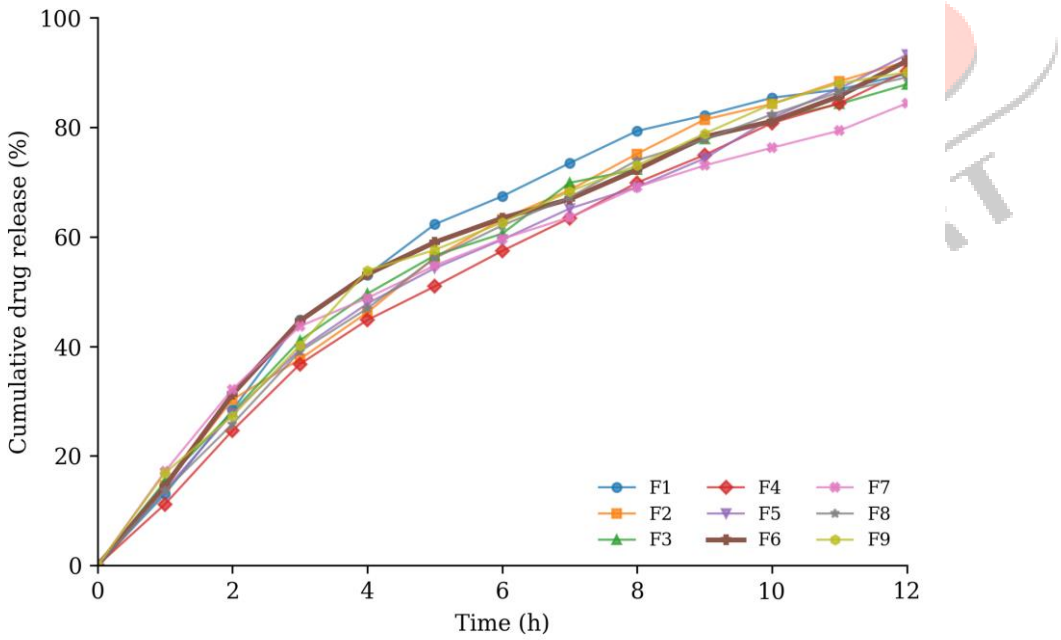

Fig. 2. In vitro cumulative drug release (%) from ethosomal batches F1–F9 over 12 h (phosphate buffer pH 7.4, 37 ± 0.5 °C).

Model	Zero-order	First-order	Higuchi	Hixson–Crowell	Korsmeyer–Peppas [60]
R^2 (batch F6)	0.9255	0.8765	0.9869	0.9833	0.6869

Table 5. Regression coefficients (R^2) of release-kinetic models for the optimized ethosomal batch (F6).

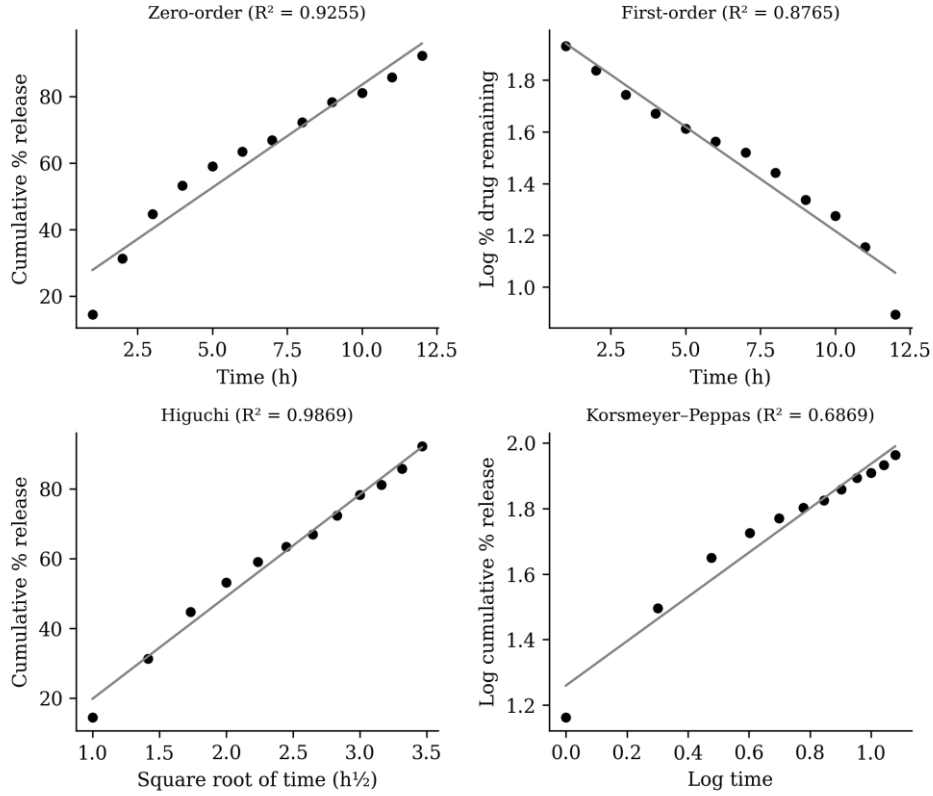

Fig. 3. Release-kinetic model fits for the optimized ethosomal batch F6: (a) zero-order, (b) first-order, (c) Higuchi and (d) Korsmeyer–Peppas plots.

3.5 Characterization and short-term stability of the optimized batch (F6)

Formulation into ethosomes markedly enhanced apparent solubility of terbinafine hydrochloride in all three media: from 9.50 to 16.56 µg/mL in distilled water, 22.66 to 46.54 µg/mL in ethanol and 17.91 to 35.67 µg/mL in phosphate buffer pH 7.4, indicating that vesicular encapsulation improves both aqueous and lipophilic-media solubility of this BCS class II drug. FTIR of the optimized ethosomes showed retention (with some broadening/reduction) of the principal terbinafine bands and no new peaks, consistent with molecular dispersion of the drug within the vesicle bilayer without chemical interaction. DSC of the optimized batch showed a broadened endothermic transition (peak 207.25 °C, onset 194.0 °C), reflecting partial loss of drug crystallinity on entrapment, consistent with successful incorporation into the lipid vesicle. [21,34,48,49]

Over one month of accelerated storage (40 ± 2 °C/75 ± 5% RH), entrapment efficiency of F6 declined only marginally, from 94.33% (day 0) to 94.22% (day 15) and 94.04% (day 30), and cumulative 12-h release changed from 92.17% to 91.98% and 91.46% over the same period (< 1% change), indicating that the optimized ethosomal suspension retained its structural integrity, entrapment and release characteristics under accelerated stress conditions.

3.6 Physicochemical evaluation of the ethosomal gel

The optimized ethosomal gel was off-white, smooth and semisolid with a slightly aromatic odour. It had a pH of 6.18, within the range compatible with normal skin pH, and a viscosity of 4125.6 cP, within the range generally accepted as stable for topical semisolids. Spreadability (38.24 g·cm/s) and extrudability (96.76%) indicated the gel could be applied and dispensed easily, and drug content uniformity of 97.89% confirmed even distribution of the active ingredient throughout the gel matrix. [55,56]

Parameter	Result
Color / odour / texture	Off-white / slightly aromatic / smooth semisolid
pH	6.18
Viscosity (cP)	4125.6
Spreadability (g·cm/s)	38.24
Extrudability (%)	96.76
Drug content uniformity (%)	97.89

Table 6. Physicochemical evaluation of the optimized terbinafine hydrochloride-loaded ethosomal gel.

In vitro release from the gel followed a biphasic pattern: an initial phase reaching ~23% release within 2 h, a rapid diffusion phase from 2–5 h (up to ~55%), and a slower sustained phase thereafter, reaching 94.76% cumulative release by 12 h (Fig. 4). This profile — a modest initial release followed by prolonged, controlled delivery — is consistent with the combined contribution of free (unentrapped) drug at the gel surface and diffusion-controlled release of vesicle-entrapped drug through the Carbopol matrix, and supports the potential for reduced dosing frequency relative to conventional gels. [55,57,59,60]

3.7 Stability of the ethosomal gel

Over one month of storage at 25 ± 2 °C/60% RH, the gel retained its organoleptic properties (off-white, smooth, slightly aromatic) at all time points. pH decreased marginally from 6.18 to 6.10, viscosity from 4125.6 to 4109.5 cP, spreadability from 38.24 to 37.63 g·cm/s, drug content from 97.89% to 97.48%, and 12-h cumulative release from 94.76% to 93.56% (Table 7, Fig. 4). All changes were small (< 2%), and the close overlap of the release profiles at 0 and 1 month confirmed that the ethosomal gel retained its physicochemical integrity and release performance over the study period, supporting adequate short-term stability under ambient storage conditions.

Parameter	Day 0	Day 15	Day 30
pH	6.18	6.15	6.10
Viscosity (cP)	4125.6	4116.5	4109.5
Spreadability (g·cm/s)	38.24	37.85	37.63
Drug content (%)	97.89	97.50	97.48
12 h cumulative drug release (%)	94.76	93.81	93.56

Table 7. One-month stability data (25 ± 2 °C/60% RH) for the optimized terbinafine hydrochloride-loaded ethosomal gel.

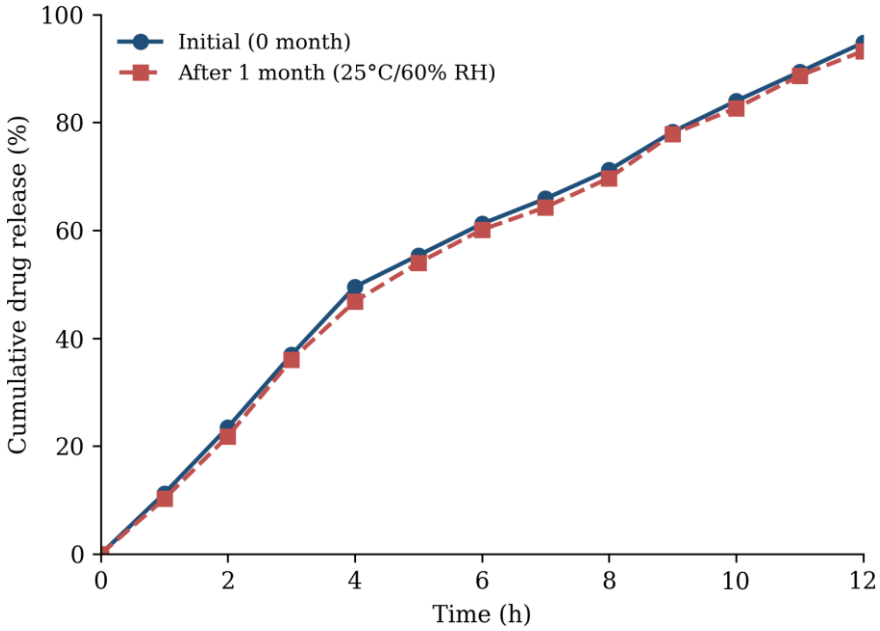

Fig. 4. In vitro cumulative drug release from the terbinafine hydrochloride ethosomal gel at initial (0 month) and after one month of storage (25 ± 2 °C/60% RH).

4. CONCLUSION

A terbinafine hydrochloride-loaded ethosomal gel was successfully developed using a 3^2 factorial design, the cold method of ethosome preparation and a Carbopol 940 gel base. The optimized ethosomal batch (F6) combined high entrapment efficiency (94.33%), nanometric and uniform particle size (235.61 nm, PDI 0.258), a strongly negative zeta potential (–38.44 mV) and diffusion-controlled (Higuchi), sustained in vitro release. Incorporation into a gel base yielded a formulation with acceptable pH, viscosity, spreadability, extrudability and drug content, biphasic sustained release over 12 h, and good short-term physicochemical stability. Collectively, these results indicate that the ethosomal gel is a technically viable, patient-friendly alternative to conventional topical antifungal vehicles for terbinafine hydrochloride, offering sustained localized delivery with the potential to reduce systemic exposure and dosing frequency. Confirmation of enhanced skin/nail permeation and antifungal efficacy will require ex vivo permeation studies, in vivo pharmacokinetic and efficacy studies, and long-term (ICH-compliant) stability data prior to clinical translation; the same ethosomal-gel platform may also be adaptable to other poorly skin-permeable antifungal or dermatological actives. [1,2,4,5,21,34]

ACKNOWLEDGEMENTS

The authors sincerely thank the Department of Pharmaceutical Quality Assurance D.S.T.S. Mandal's college of Pharmacy, Solapur, for providing the necessary laboratory facilities and support to carry out this research work.

CONFLICT OF INTEREST

The authors declare no conflict of interest.

REFERENCES

1. Priya, S., Shridhar, P., Shekhara, K., Shenthar, S., & Kudva, S. K. (2025). Tolnaftate-loaded ethosomal gel for topical delivery: Formulation and in vitro evaluation. Journal of Health and Allied Sciences NU, 15(01), 026-031.
2. Dhurve, R., Kashyap, N., Mishra, A., & Pathak, A. K. (2014). A holistic review on ethosome: a promising drug delivery system for topical fungal disease. Int J Pharm Biol Arch, 5(05), 13-26.
3. Rakesh, R., & Anoop, K. R. (2012). Ethosomes for transdermal and topical drug delivery. Int J Pharm Pharm Sci, 4(3), 17-24.
4. Bhalaria, M. K., Naik, S., & Misra, A. N. (2009). Ethosomes: A novel delivery system for antifungal drugs in the treatment of topical fungal diseases.
5. Indora, N., & Kaushik, D. (2015). Design, development and evaluation of ethosomal gel of fluconazole for topical fungal infection. International Journal of Engineering Science Invention Research & Development, 1(8), 280-306.
6. Sujitha, B., Krishnamoorthy, B., & Muthukumaran, M. (2014). Formulation and evaluation of piroxicam loaded ethosomal gel for transdermal delivery. Int J Adv Pharm Gen Res, 2(1), 34-45.
7. Paliwal, S., Tilak, A., Sharma, J., Dave, V., Sharma, S., Yadav, R., ... & Tak, K. (2019). Flurbiprofen loaded ethosomes-transdermal delivery of anti-inflammatory effect in rat model. Lipids in Health and Disease, 18, 1-15.
8. Abousamra, M. M., & Mohsen, A. M. (2016). Solid lipid nanoparticles and nanostructured lipid carriers of tolnaftate: Design, optimization and in-vitro evaluation. Int. J. Pharm. Pharm. Sci, 10, 100.
9. Almuqbil, R. M., & Aldhubiab, B. (2025). Ethosome-based transdermal drug delivery: Its structural components, preparation techniques and therapeutic applications across metabolic, chronic and oncological conditions. Pharmaceutics, 17(5), 583.
10. Shukla, T., Verma, A., Upmanyu, N., Mishra, S. S., & Shilpi, S. (2016). Development and characterization of clopidogrel-loaded ethosomal transdermal patch for antiplatelet effect. Asian J Pharm, 10(4), 1-7.
11. Nagadevi, B., Kumar, K. S., Venkanna, P., & Prabhakar, D. (2014). Formulation and characterization of tizanidine hydrochloride loaded ethosomes patch. Int J Pharm Pharm Sci, 6(4), 199-205.
12. Irfan, M., Verma, S., & Ram, A. (2012). Preparation and characterization of ibuprofen loaded transferosome as a novel carrier for transdermal drug delivery system. Asian Journal of Pharmaceutical and Clinical Research, 5(3), 162-165.
13. Duangjit, S., Opanasopit, P., Rojanarata, T., & Ngawhirunpat, T. (2011). Characterization and in vitro skin permeation of meloxicam-loaded liposomes versus transfersomes. Journal of Drug Delivery, 2011(1), 418316.
14. Kumar, M. S. (2014). Development of celecoxib transfersomal gel for the treatment of rheumatoid arthritis. Indian Journal of Pharmaceutical and Biological Research, 2(2).
15. Hamblin, M. R., Avci, P., & Prow, T. (Eds.). (2016). Nanoscience in Dermatology. Academic Press.
16. Ar, H. (1993). Cell death by apoptosis in epidermal biology. J Invest Dermatol, 101, 107-112.
17. Murphy, G. F. (1997). Histology of the skin. Lever's Histopathology of the Skin, 43-45.
18. Agrawal, U., Mehra, N. K., Gupta, U., & Jain, N. K. (2013). Hyperbranched dendritic nano-carriers for topical delivery of dithranol. Journal of Drug Targeting, 21(5), 497-506.
19. Ainbinder, D., & Touitou, E. (2005). Testosterone ethosomes for enhanced transdermal delivery. Drug Delivery, 12(5), 297-303.

20. Babu, R. J., Kanikkannan, N., Kikwai, L., Ortega, C., Andega, S., Ball, K., ... & Singh, M. (2003). The influence of various methods of cold storage of skin on the permeation of melatonin and nimesulide. Journal of Controlled Release, 86(1), 49-57.

21. Touitou, E., Dayan, N., Bergelson, L., Godin, B., & Eliaz, M. (2000). Ethosomes—novel vesicular carriers for enhanced delivery: characterization and skin penetration properties. Journal of Controlled Release, 65(3), 403-418.

22. Rekha, B. (2018). Formulation and characterization of atorvastatin ethosomal gel. J Drug Dev Del, 1(1), 13-20.

23. Indira, S., Priyanka, R., & Prathima, S. (2015). Formulation and evaluation of ethosomal topical gels of etoricoxib. International Journal for Pharmaceutical Research Scholars, 4(1), 93-103.

24. Bala, T. S. (2017). Formulation and in vitro evaluation of topical ethosomal gels of miconazole nitrate. World J Pharm Pharm Sci, 6(8), 1882-1898.

25. Rathore, A. R., Khambete, H., & Jain, S. (2013). Preparation and characterization of repaglinide loaded ethosomal gel for the treatment of NIDDM. Int J Pharm Biol Arch, 4(2), 385-390.

26. Acharya, A., Ahmed, M. G., & Rao, B. D. (2016). Development and evaluation of ethosomal gel of lornoxicam for transdermal delivery: in-vitro and in-vivo evaluation. Manipal Journal of Pharmaceutical Sciences, 2(1), 3.

27. Shivhare, U. D., Jain, K. B., Mathur, V. B., Bhusari, K. P., & Roy, A. A. (2009). Formulation development and evaluation of diclofenac sodium gel using water soluble polyacrylamide polymer. Digest Journal of Nanomaterials & Biostructures, 4(2).

28. Panigrahi, L., John, T., Shariff, A., & Hiremath, S. R. R. (1997). Formulation and evaluation of lincomycin HCl gels. Indian Journal of Pharmaceutical Sciences, 59(6), 330-332.

29. Bhalekar, M. R., Pokharkar, V., Madgulkar, A., Patil, N., & Patil, N. (2009). Preparation and evaluation of miconazole nitrate-loaded solid lipid nanoparticles for topical delivery. AAPS PharmSciTech, 10, 289-296.

30. Alkhalidi, H. M., Hosny, K. M., & Rizg, W. Y. (2020). Oral gel loaded by fluconazole-sesame oil nanotransfersomes: development, optimization and assessment of antifungal activity. Pharmaceutics, 13(1), 27.

31. Saifee, M., Atre, M., & Toshniwal, R. (2021). Formulation and in-vitro evaluation of ethosomal gel of repaglinide for transdermal delivery. Int J Pharm Phytopharmacol Res, 11(4), 11-17.

32. Garg, B. J., Garg, N. K., Beg, S., Singh, B., & Katare, O. P. (2016). Nanosized ethosomes-based hydrogel formulations of methoxsalen for enhanced topical delivery against vitiligo: formulation optimization, in vitro evaluation and preclinical assessment. Journal of Drug Targeting, 24(3), 233-246.

33. Anju, K., Priya, S., Sandeep, D. S., Nayak, P., Kumar, P., Kumar, A., ... & Krithi, S. P. (2021). Formulation and optimization of zaltoprofen loaded ethosomal gel using a 2^3 full factorial design.

34. Sinico, C., & Fadda, A. M. (2009). Vesicular carriers for dermal drug delivery. Expert Opinion on Drug Delivery, 6(8), 813-825.

35. Shamma, R. N., & Elsayed, I. (2013). Transfersomal lyophilized gel of buspirone HCl: formulation, evaluation and statistical optimization. Journal of Liposome Research, 23(3), 244-254.

36. Khan, R. A., Saif, A., Naureen, H., Sarwar, A., Shahbaz, M. A., & Arif, M. N. (2022). Formulation and evaluation of metronidazole loaded nanosponges for topical delivery. Pharmaceutical Communications, 1(01), 71-87.

37. Singh, S., Verma, D., Mirza, M. A., Das, A. K., Anwer, M. K., Sultana, Y., ... & Iqbal, Z. (2017). Development and optimization of ketoconazole loaded nano-transfersomal gel for vaginal delivery using Box-Behnken design: In vitro, ex vivo characterization and antimicrobial evaluation. Journal of Drug Delivery Science and Technology, 39, 95-103.

38. Abdellatif, K. R., & Fadaly, W. A. (2017). New 1,2-diaryl-4-substituted-benzylidene-5-4H-imidazolone derivatives: Design, synthesis and biological evaluation as potential anti-inflammatory and analgesic agents. Bioorganic Chemistry, 72, 123-129.

39. Qushawy, M., Nasr, A., Abd-Alhaseeb, M., & Swidan, S. (2018). Design, optimization and characterization of a transfersomal gel using miconazole nitrate for the treatment of candida skin infections. Pharmaceutics, 10(1), 26.

40. Khalid, R., Mahmood, S., Sofian, Z. M., Chik, Z., & Ge, Y. (2025). Development of rapidly dissolving microneedles integrated with valsartan-loaded nanoliposomes for transdermal drug delivery: In vitro and ex vivo evaluation. Pharmaceutics, 17(4), 483.

41. Cheng, Z., Kandekar, U., Ma, X., Bhabad, V., Pandit, A., Liu, L., ... & Tao, L. (2024). Optimizing fluconazole-embedded transfersomal gel for enhanced antifungal activity and compatibility studies. Frontiers in Pharmacology, 15, 1353791.

42. Bostancı, F., Şengelen, A., Aksüt, Y., Yıldırım, E., Öğütcü, İ., Yücel, O., ... & Pekmez, M. (2025). Indomethacin-encapsulated PLGA nanoparticles improve therapeutic efficacy by increasing apoptosis and reducing motility in glioblastoma cells. Pharmaceutical Development and Technology, 30(1), 25-36.

43. Opatha, S. A. T., Chutoprapat, R., Khankaew, P., Titapiwatanakun, V., Ruksiriwanich, W., & Boonpisuttinant, K. (2024). Asiatic acid-entrapped transfersomes for the treatment of hypertrophic scars: In vitro appraisal, bioactivity evaluation and clinical study. International Journal of Pharmaceutics, 651, 123738.

44. Balasubramanyam, P., Sudheer, P., Sreeharsha, N., Nair, A. B., & Ramachandra, D. P. (2025). Transfersomes mediated transdermal delivery of curcumin: In vitro and in vivo evaluation. Pharmaceutical Sciences, 31(2), 203-215.

45. Weisberg, S. (2015). Linear Hypothesis: Regression (basics).

46. Fadodun, O. G., Amosun, A. A., Salau, A. O., Olaloye, D. O., Ogundeji, J. A., Ibitoye, F. I., & Balogun, F. A. (2020). Numerical investigation and sensitivity analysis of turbulent heat transfer and pressure drop of Al2O3/H2O nanofluid in a straight pipe using response surface methodology. Archives of Thermodynamics, 41(1), 3-30.

47. Clarke, B. R. (2008). Linear Models: The Theory and Application of Analysis of Variance. John Wiley & Sons.

48. Abd El-Alim, S. H., Kassem, A. A., Basha, M., & Salama, A. (2019). Comparative study of liposomes, ethosomes and transfersomes as carriers for enhancing the transdermal delivery of diflunisal: In vitro and in vivo evaluation. International Journal of Pharmaceutics, 563, 293-303.

49. Ashtikar, M., Nagarsekar, K., & Fahr, A. (2016). Transdermal delivery from liposomal formulations—Evolution of the technology over the last three decades. Journal of Controlled Release, 242, 126-140.

50. Bhatia, K. S., Gao, S., & Singh, J. (1997). Effect of penetration enhancers and iontophoresis on the FT-IR spectroscopy and LHRH permeability through porcine skin. Journal of Controlled Release, 47(1), 81-89.

51. Lopes, J., Correia, M., Martins, I., Henriques, A. G., Delgadillo, I., da Cruz e Silva, O., & Nunes, A. (2016). FTIR and Raman spectroscopy applied to dementia diagnosis through analysis of biological fluids. Journal of Alzheimer's Disease, 52(3), 801-812.

52. Obata, Y., Utsumi, S., Watanabe, H., Suda, M., Tokudome, Y., Otsuka, M., & Takayama, K. (2010). Infrared spectroscopic study of lipid interaction in stratum corneum treated with transdermal absorption enhancers. International Journal of Pharmaceutics, 389(1-2), 18-23.

53. Wallach, D. F., Verma, S. P., & Fookson, J. (1979). Application of laser Raman and infrared spectroscopy to the analysis of membrane structure. Biochimica et Biophysica Acta (BBA)-Reviews on Biomembranes, 559(2-3), 153-208.

54. Yang, H., Wu, X., Zhou, Z., Chen, X., & Kong, M. (2019). Enhanced transdermal lymphatic delivery of doxorubicin via hyaluronic acid based transfersomes/microneedle complex for tumor metastasis therapy. International Journal of Biological Macromolecules, 125, 9-16.

55. Shruthi, K. A. (2023). Review: Pharmaceutical gels and its types with prominence role of its drug delivery systems. IJRAR, 10, 686.

56. Flynn, G. L., Linn, E. E., Kurihara-Bergstrom, T., Govil, S. K., & Hou, S. Y. E. (1987). Parameters of skin condition and function. Transdermal Delivery of Drugs, 2, 3-17.

57. Peppas, N. A. (1985). Analysis of Fickian and non-Fickian drug release from polymers. Pharmaceutica Acta Helvetiae, 60(4), 110-111.

58. Schwartz, J. B., Simonelli, A. P., & Higuchi, W. I. (1968). Drug release from wax matrices I. Analysis of data with first-order kinetics and with the diffusion-controlled model. Journal of Pharmaceutical Sciences, 57(2), 274-277.

59. Higuchi, T. (1963). Mechanism of sustained-action medication. Theoretical analysis of rate of release of solid drugs dispersed in solid matrices. Journal of Pharmaceutical Sciences, 52(12), 1145-1149.

60. Korsmeyer, R. W., Gurny, R., Doelker, E., Buri, P., & Peppas, N. A. (1983). Mechanisms of solute release from porous hydrophilic polymers. International Journal of Pharmaceutics, 15(1), 25-35.

61. D'souza, J. I., & More, H. N. (2008). Topical anti-inflammatory gels of fluocinolone acetonide entrapped in Eudragit-based microsponge delivery system. Research Journal of Pharmacy and Technology, 1(4), 502-506.